

## Preparation of Thermostable and Electroconductive PANI/TDI-CeO<sub>2</sub> Composite by Graft Polymerization and its Electrochemical Properties

Yang Fei<sup>1,3</sup>, Hui Huang<sup>1,3,\*</sup>, Shuang Song<sup>1,3</sup>, Lei Jin<sup>1,3</sup>, Xiaojun Zhang<sup>1,3</sup>, Zhongcheng Guo<sup>1,2,3</sup>

<sup>1</sup> Faculty of Metallurgical and Energy Engineering, Kunming University of Science & Technology, Kunming 650093, PR China

<sup>2</sup> Kunming Hendera Science & Technology Co. Ltd., Kunming 650106, PR China

<sup>3</sup> Yunnan Provincial Engineering Technology Research Center of Metallurgical Electrode Materials, Kunming 650106, PR China

\*E-mail: [huihuanghan@163.com](mailto:huihuanghan@163.com)

Received: 9 July 2017 / Accepted: 24 August 2017 / Published: 28 December 2017

Electroconductive polymer/inorganic particle composites have been found to have unique physiochemical properties and important application value in many fields. However, previously reported composites are of low thermostability and poor electroconductivity. Here in the article, a novel hybrid composite of PANI/CeO<sub>2</sub>-TDI was proposed to overcome those shortcomings. Firstly, cerium dioxide (CeO<sub>2</sub>) was successfully modified by toluene-2,4-diisocyanate (TDI) via the addition reaction between TDI molecules and -OH groups at the CeO<sub>2</sub> particles' surface. The reactive -NCO groups at the surface of those modified particles further reacted with polyaniline (PANI) by graft polymerization to give the target composite, whose structure is characterized by FTIR and XRD, respectively. The thermogravimetric analysis (TGA) was used to characterize the thermal stability of obtained composites, and their electrochemical performances were characterized by rotating disc electrode (RDE) method in an electrolyte solution of 150 g/L H<sub>2</sub>SO<sub>4</sub> and 65 g/L Zn<sup>2+</sup> at 35 °C. The results showed that the target composite starts decomposing at about 260 °C which is the highest compared with control samples (pure PANI (~215 °C) and PANI/CeO<sub>2</sub> (~226 °C)), has the lowest static oxygen evolution potential (1.78 V vs MSE) compared with pure PANI (1.92 V, vs MSE) and PANI/CeO<sub>2</sub> (1.84 V, vs MSE) as well as the dynamic oxygen evolution potential as shown in the measured anodic polarization curves, possesses the largest electrode surface current density (2.9x10<sup>-4</sup> A·cm<sup>-2</sup>) compared with pure PANI (7.3x10<sup>-5</sup> A·cm<sup>-2</sup>) and PANI/CeO<sub>2</sub> (1.2x10<sup>-4</sup> A·cm<sup>-2</sup>), and also owns the largest reaction rate constant (1.39x10<sup>12</sup> m·s<sup>-1</sup>).

**Keywords:** Cerium dioxide, toluene-2,4-diisocyanate, graft polymerization, polyaniline, rotating disk electrode(RDE)

## 1. INTRODUCTION

Recently, electroconductive polymer/inorganic-particle composites have been found to have excellent physiochemical properties and have many potential applications in new technologies. For instance, they have been reported being able to be used as electrocatalysts, chemosensors, conductive coatings, charge storages, and battery materials[1].

Being of high conductivity, excellent stability, and easiness of manufacturing of electronic devices and chemosensors[2-4], polyaniline (PANI) which is one of the electroconductive organic polymers, has been studied intensively. Meanwhile, among those inorganic materials, cerium (Ce) is the most representative, whose electron configuration is  $[\text{Xe}]4f^26s^2$ . It has two common oxidation states, cerium(IV) and cerium(III). Technologically, Cerium dioxide ( $\text{CeO}_2$ ) is very important because it can be used as a catalyst to eliminate auto-exhaust gases and to promote water-gas shift reaction, can be used as a sensitive membrane to transport or detect oxygen, and can be used as ultraviolet absorbent[5-8].

There are many composites of PANI and  $\text{CeO}_2$  prepared by a variety of methods. E. Kumar's team obtained PANI/ $\text{CeO}_2$  nanocomposites via in-situ polymerization of aniline with  $\text{CeO}_2$  nanoparticles in the reaction system[9]. Zhang Jun-Qing's group synthesized PANI/ $\text{CeO}_2$  composite particles, indicating that PANI/ $\text{CeO}_2$  composite was irregular in shape, and the size distribution was multimodal[10]. Feng-Yi Chuang's team got a  $\text{CeO}_2$ /PANI core-shell nanocomposite via oxidation of aniline in which  $\text{CeO}_2$  was used as oxidant[11]. In all the above cases,  $\text{CeO}_2$  particles physically absorb PANI to form a coating, which makes those composites have poor thermostability.

Herein, we expect that composites that have excellent thermostability and electrocatalytic activity while maintaining the electrochemical properties of its substrate can be prepared by an indirect chemical bonding of PANI to  $\text{CeO}_2$  surface. That is, by using one -NCO group of difunctional toluene-2,4-diisocyanate (TDI) to form a bond with one -OH group at  $\text{CeO}_2$  particles' surface and the other -NCO group to form a bond with - $\text{NH}_2$  group from aniline (AN), then a graft polymerization is induced to give PANI/ $\text{CeO}_2$ -TDI composites, whose structural and electrochemical properties were characterized by FTIR, XRD, TGA, and RDE.

## 2. EXPERIMENTAL AND METHODS

### 2.1. Materials

Aniline was purchased from Shanghai Chemical Works, distilled under reduced pressure, and used as the monomer. Sulfosalicylic acid (SSA) and Ammonium persulfate (APS) were used as dopant and oxidant, respectively. Toluene-2,4-diisocyanate (TDI) and Carbon Tetrachloride ( $\text{CCl}_4$ ) were obtained from Chengdu Xiya Reagent Co. Ltd. They were stored at low-temperature before use. Cerium dioxide ( $\text{CeO}_2$ ) whose average particle size is 1  $\mu\text{m}$  was purchased from Shanghai ST-Nano science and technology Co. Ltd. Nafion solution was obtained from Shanghai Hesen Co. Ltd. Other chemicals used in the experiment were of AR grade.

## 2.2. Synthesis of PANI/CeO<sub>2</sub>-TDI Composites

The strategy to prepare PANI/CeO<sub>2</sub>-TDI composites includes three major steps. The first step is to modify CeO<sub>2</sub> particle with TDI to prepare CeO<sub>2</sub>-TDI composite. The next step is to prepare CeO<sub>2</sub>-TDI-An via the reaction between CeO<sub>2</sub>-TDI and aniline. The last step is to graft PANI to the surface of CeO<sub>2</sub>-TDI-An.

In the first step, the functionalization process was performed as follows: 3.0 g of CeO<sub>2</sub> particles and 3.12 g of TDI was dispersed in 80 mL of dried CCl<sub>4</sub> and ultrasonically bathed for 30 min. Then the reaction mixture was magnetically stirred and maintained at 80 °C for 12 h. The reaction product was washed with CCl<sub>4</sub>, separated by centrifugation to remove the excessive TDI, and dried under vacuum at 60 °C for 24 h to obtain the anhydrous CeO<sub>2</sub>-TDI composite.

In the second step, 0.4 g CeO<sub>2</sub>-TDI particles were dispersed into 25 mL solution of dried CCl<sub>4</sub> and aniline for 30 min. Afterward, the product, CeO<sub>2</sub>-TDI-An, was washed with CCl<sub>4</sub> and dried under vacuum at 60 °C for 24 h.

In the third step, there are five substeps. First of all, about 1.325 g of SSA was dissolved in 1600 mL of H<sub>2</sub>SO<sub>4</sub> and continually stirred for 2 h to obtain SSA solution. Secondly, 400 mL of the SSA solution was used to disperse 1.875 g CeO<sub>2</sub>-TDI-An particles with ultrasonic bath for 15 min. Thirdly, another 400 mL of SSA solution was used to dissolve 25 mL of distilled An with magnetic stirring for 1 h, and the mixture was blended with the solution prepared in the first step with strong stirring for about 1 h. Fourthly, the left 600 mL of SSA solution was used to dissolve 5.475 g of APS, and the obtained solution was added to the solution prepared in the previous step drop by drop, and the reaction was kept at 5~10 °C for 6 hours with constant stirring speed. Finally, the PANI/CeO<sub>2</sub>-TDI composite was filtered, washed, and dried at 60 °C.

To make a contrast to the prepared PANI/CeO<sub>2</sub>-TDI composites, the synthesis of pure PANI and PANI/CeO<sub>2</sub> were similar.

## 2.3. Modification of electrode

The catalyst ink was prepared by dispersing 10 mg of PANI/CeO<sub>2</sub>-TDI in 950 μL of ethanol, and the solution was mixed with 50 μL of 5 wt% Nafion solution with ultrasonic bath for 30 min. 10 μL of the suspension was clung to glassy carbon disk (5.0 mm diameter) and dried at the temperature of 60 °C under vacuum. The prepared electrode was noted as PANI/CeO<sub>2</sub>-TDI/GC. The process for PANI/GC and PANI/CeO<sub>2</sub>/GC followed the same procedure.

## 2.4. Characterization of composites

The X-ray diffraction measurements were performed by XRD (D/max-3BX, Japan) with Ni-filtered Cu K $\alpha$  radiation. The FTIR spectra of the samples (KBr pellets method) were measured with the spectral range of 4000 ~ 400 cm<sup>-1</sup> using FTIR (PK6000, USA). Thermogravimetric analysis (TGA) was carried out on a Shimadzu DT-20 from 0 °C up to 700 °C, in which the heating rate is 20 °C min<sup>-1</sup> in the air.

Rotating disk electrode (RDE) voltammetry was tested in a single three-electrode system in which cyclic voltammetry, anodic polarization curves, and Tafel polarization curves of the modified electrode were also measured. The electrolyte used was of  $150 \text{ g}\cdot\text{L}^{-1} \text{H}_2\text{SO}_4$  and  $65 \text{ g}\cdot\text{L}^{-1} \text{Zn}^{2+}$  at  $35 \text{ }^\circ\text{C}$ . The working electrode was the modified electrode, and its working areas were  $0.196 \text{ cm}^2$ . A  $\text{Hg}/\text{Hg}_2\text{SO}_4$  ( $\text{K}_2\text{SO}_4$ , saturated) electrode and a platinum wire were used as the reference electrode and auxiliary electrode, respectively. Those measurements were carried out at the electrochemical workstation CS350.

### 3. RESULTS AND DISCUSSION

#### 3.1. FTIR Analysis

Figure 1 depicts the FTIR spectra of  $\text{CeO}_2$ ,  $\text{CeO}_2$ -TDI,  $\text{CeO}_2$ -TDI-An, PANI, PANI/ $\text{CeO}_2$ -TDI hybrids, and PANI/ $\text{CeO}_2$  composites. It can be found in Figure 1 (Curve b) that except the bands of pristine  $\text{CeO}_2$ , the TDI functionalized  $\text{CeO}_2$  ( $\text{CeO}_2$ -TDI) exhibited several characteristic bands in which the band at  $2275 \text{ cm}^{-1}$  is ascribed to the ortho-isocyanate groups of TDI attached to the  $\text{CeO}_2$  surface while the peaks at  $1646 \text{ cm}^{-1}$  and  $1599 \text{ cm}^{-1}$  can be assigned to the newly formed -CONH-group, the band at  $1550 \text{ cm}^{-1}$  can be attributed to the phenyl ring of TDI[12]. Those bands clearly showed that the covalent bonds were formed between TDI molecules and  $\text{CeO}_2$  particles, implying the surface functionalization of the  $\text{CeO}_2$  particle with TDI was successful. In Figure 1 (Curve c), the peak at  $2275 \text{ cm}^{-1}$  disappeared, which can be assigned to the reaction between an ortho-isocyanate group on the  $\text{CeO}_2$  surface and an amino group in aniline.

The primary characteristic peaks of the pure PANI (Figure 1d) can be assigned as follows: the band at  $3441 \text{ cm}^{-1}$  can be attributed to N-H stretching mode; the bands at  $1560 \text{ cm}^{-1}$  and  $1477 \text{ cm}^{-1}$  are attributable to C=N stretching mode of quinonoid and C=C stretching mode of benzenoid units, respectively; and C-N stretching mode of benzenoid unit occurs at  $1298 \text{ cm}^{-1}$  and  $1237 \text{ cm}^{-1}$ , while the bands at  $1124 \text{ cm}^{-1}$  and  $808 \text{ cm}^{-1}$  are attributable to the in-plane bending vibration of C-H (modes of  $\text{Q}=\text{N}^+\text{H}-\text{B}$ ,  $\text{N}=\text{Q}=\text{N}$ , and  $\text{B}-\text{N}^+\text{H}-\text{B}$ ) where Q and B represent the quinoid and benzenoid units, and C-H bending mode of aromatic rings[13]. The characteristic peaks of composite PANI/ $\text{CeO}_2$  (Figure 1f) are almost the same as those of pure PANI, which implies in the composite PANI/ $\text{CeO}_2$ , the molecular structure of PANI is consistent with the pure PANI and there is no strong interaction between PANI and  $\text{CeO}_2$ .

The FTIR of PANI/ $\text{CeO}_2$ -TDI composite (Figure 1e) also shows similar characteristic peaks. For instance, the corresponding peaks of PANI/ $\text{CeO}_2$ -TDI composite at  $1577 \text{ cm}^{-1}$  shifted from  $1560 \text{ cm}^{-1}$ ,  $1497 \text{ cm}^{-1}$  shifted from  $1477 \text{ cm}^{-1}$ ,  $1308 \text{ cm}^{-1}$  shifted from  $1298 \text{ cm}^{-1}$ ,  $1240 \text{ cm}^{-1}$  shifted from  $1237 \text{ cm}^{-1}$ ,  $1127 \text{ cm}^{-1}$  shifted from  $1124 \text{ cm}^{-1}$  in pure PANI. Those blue shifts imply that there is strong interaction between PANI and  $\text{CeO}_2$ -TDI via graft polymerization.

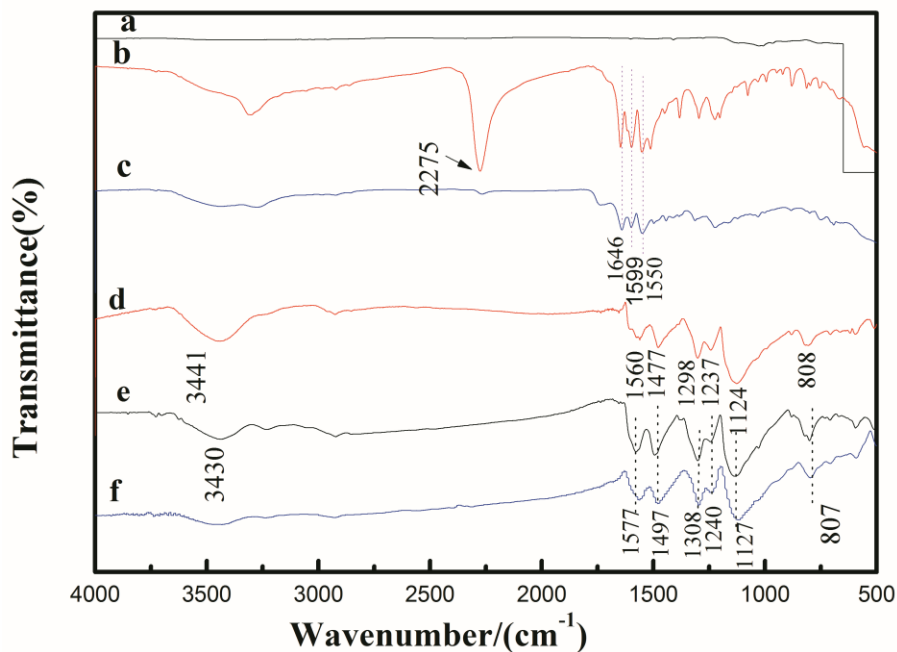


**Figure 1.** FTIR spectra of samples: (a)  $\text{CeO}_2$ , (b)  $\text{CeO}_2$ -TDI, (c)  $\text{CeO}_2$ -TDI-An, (d) PANI, (e) PANI/ $\text{CeO}_2$ -TDI and (f) PANI/ $\text{CeO}_2$

### 3.2. X-Ray diffraction analysis

The XRD patterns of the  $\text{CeO}_2$ ,  $\text{CeO}_2$ -TDI, PANI, PANI/ $\text{CeO}_2$ -TDI and PANI/ $\text{CeO}_2$ , are shown in Figure 2. The XRD pattern of  $\text{CeO}_2$  particles typically presents the cubic structure without extra reflections (Figure 2 curve (a)), and it can be well indexed to (111), (200), (220), (311), (222), (400), (331), (420) and (422) crystal plane of cubic  $\text{CeO}_2$  (JCPDS Card No.34-0394). Comparing curve (b) with the curve (a), it can be observed that the diffraction pattern of TDI-modified  $\text{CeO}_2$  is the same with that of pristine  $\text{CeO}_2$ , which implies that surface modification with TDI has no effect on the crystal structure of the  $\text{CeO}_2$  particle. As shown in Figure 2 (c), there are two broad diffraction peaks centered at  $2\theta=19.6^\circ$  and  $24.9^\circ$ , which are attributable to the periodically parallel and perpendicular plane to the polymer chains of pure PANI, respectively[14]. However, when PANI and  $\text{CeO}_2$  particles form complexes, the diffraction peak of  $\text{CeO}_2$  almost disappears. This fact indicates that polyaniline coated on the unmodified  $\text{CeO}_2$  will affect the crystal form of  $\text{CeO}_2$ . Figure 2 (d) depicts the XRD pattern of PANI/ $\text{CeO}_2$ -TDI composites. It includes the characteristic peaks of  $\text{CeO}_2$ , suggesting that  $\text{CeO}_2$  is a good carrier for the stable existence of PANI in the process of aniline polymerization. The intensity of the broad diffraction peaks of PANI in the composite becomes weaker after introducing  $\text{CeO}_2$ -TDI, which suggests that  $\text{CeO}_2$ -TDI particles affect the crystallinity of PANI. In addition, the significant differences in the order and crystallinity of PANI composite, molecular chain increasing, structural defects reducing, and energy gap decreasing indicate that the conductivity of the composite is electrochemically improved[15]. This result also shows the interaction between polymer chains of PANI and  $\text{CeO}_2$ -TDI particles is due to the forming of covalent bonds.

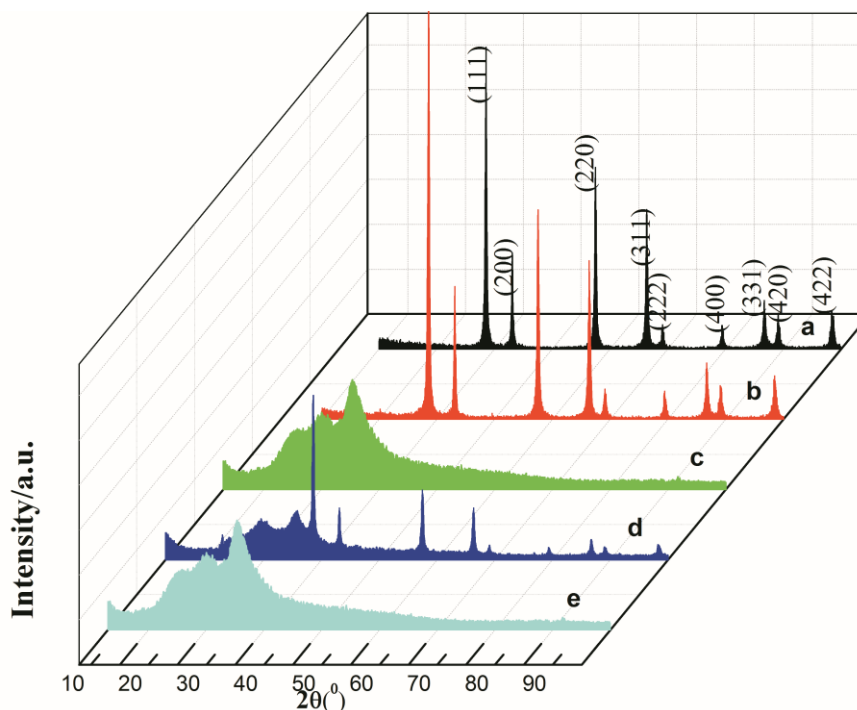


**Figure 2.** XRD pattern of the samples: (a)  $\text{CeO}_2$  particles, (b)  $\text{CeO}_2$ -TDI, (c) PANI, (d) PANI/  $\text{CeO}_2$ -TDI and (e) PANI/ $\text{CeO}_2$

### 3.3. TGA analysis

TGA analysis was used to characterize the thermal properties of TDI-modified  $\text{CeO}_2$  ( $\text{CeO}_2$ -TDI), PANI, PANI/ $\text{CeO}_2$ -TDI and PANI/ $\text{CeO}_2$ , as shown in Figure 3.

The thermal decomposition curve of  $\text{CeO}_2$ -TDI hybrids (Figure 3 curve (a)) shows two-stage decomposition pattern. The weight loss of sample at temperatures below about 100 °C is due to the loss of water molecules, which is fairly slower from 100 °C to 200 °C. The weight loss increases rapidly in the temperature range of 200~700 °C, which is mainly attributed to the loss of TDI molecules covalently attached to the  $\text{CeO}_2$  surface. In the temperature, all the TDI molecules are actually decomposed completely. It can be found in Figure 3 (curve a) that the weight loss amounted to 23% in the temperature range of 100-700 °C, which is attributable to weight loss of  $\text{CeO}_2$ -TDI.

The weight loss of pure PANI (Figure 3, curve (c)) at the temperature range of 20 °C~120 °C is mainly due to the moisture and eliminated impurities, and the pure PANI exhibits a sharp decrease in mass (about 84%) at the at temperatures range of 180 °C~600 °C. The sharp decrease is caused by decomposition of pure PANI. However, the mass loss of PANI/ $\text{CeO}_2$ -TDI (Figure 3, curve (d)) from 245 °C~600 °C is about 70%, and the initial decomposition temperature (~260 °C) is the highest when compared to the pristine PANI (~245 °C) and composite PANI/ $\text{CeO}_2$  (~219 °C). Therefore, the PANI/ $\text{CeO}_2$ -TDI composite has excellent thermostability, which might be due to the interaction between  $\text{CeO}_2$ -TDI and the inter-chains in PANI macromolecule.

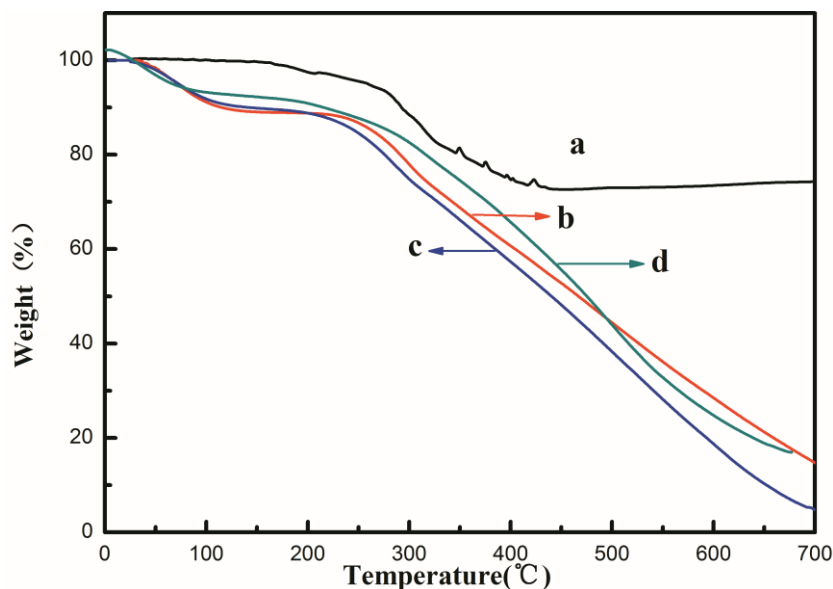


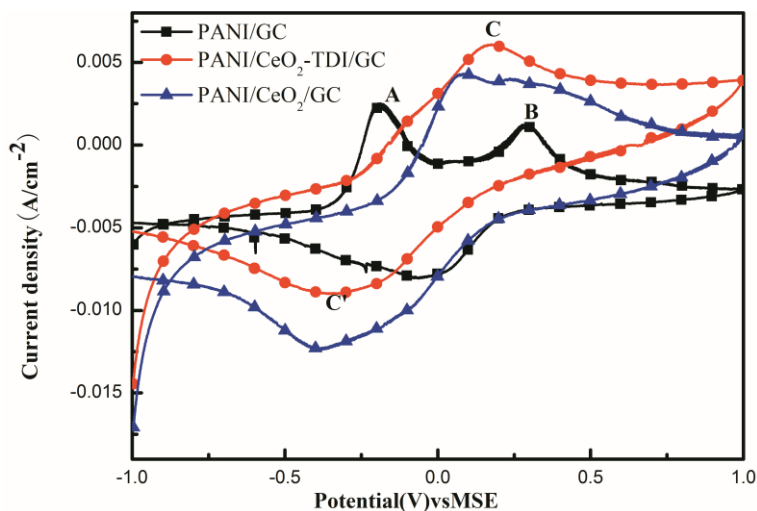
**Figure 3.** TGA curves of (a) CeO<sub>2</sub>-TDI, (b) PANI/ CeO<sub>2</sub>, (c) PANI and (d) PANI/CeO<sub>2</sub>-TDI

### 3.4. Electrochemical properties

The cyclic voltammetry, anodic polarization, and Tafel polarization for modified electrode are measured in an electrolyte of 150 g/L H<sub>2</sub>SO<sub>4</sub> and 65 g/L Zn<sup>2+</sup> and at 35 °C.

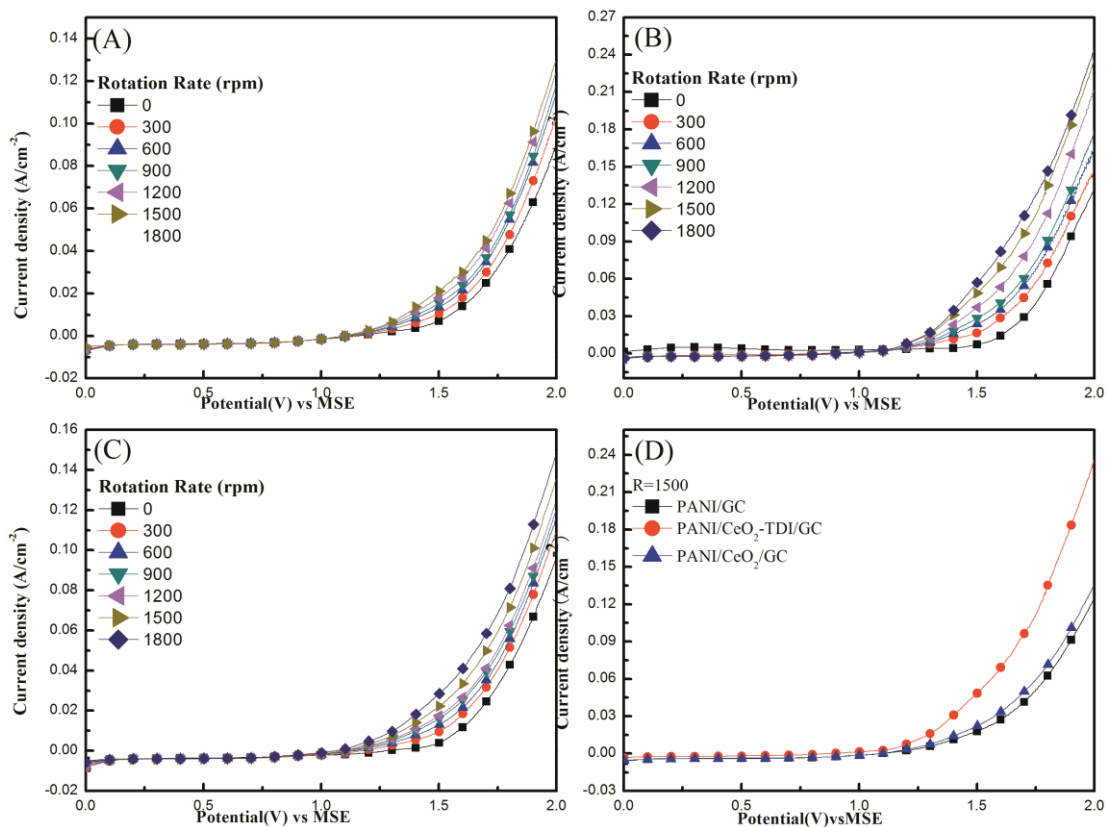
#### 3.4.1. Cyclic voltammetry

Fig.4 shows the different modified electrodes' electrochemical activity in an electrolyte of 150 g/L H<sub>2</sub>SO<sub>4</sub> and 65 g/L Zn<sup>2+</sup>. The scan rate is 10 mV/s. As shown in Fig.4, the characteristics of the redox reaction of PANI are two redox pairs with oxidation peaks of PANI/GC modified electrode, peak A and B, located at -0.1 V and 0.3 V, respectively. The peak A corresponds to the first oxidation step of neutral PANI, and the peak B represents the further oxidation of PANI, from emeraldine to nigraniline[16]. The peak current of PANI/CeO<sub>2</sub>/GC electrode is higher than that of PANI/GC electrode in the cyclic voltammetry curve, indicating that the composites between inorganic particles CeO<sub>2</sub> and PANI will affect both the electroactivity and capacitance characteristics of PANI. Herein the CV of PANI/CeO<sub>2</sub>-TDI/GC modified electrode are characterized by a single redox pair CC', with broad anodic and cathodic curves, and it is evident from peak C that PANI/CeO<sub>2</sub>-TDI/GC modified electrode possesses larger peak current and better electrochemical activity compared with PANI/GC modified electrode. That fact indicates that the composites with the covalent bond between PANI and CeO<sub>2</sub> by introducing TDI can improve the performance of pure PANI, which is attributable to the electrostatic interaction between the chemically flexible NH group of PANI and the TDI-functionalized CeO<sub>2</sub>.



**Figure 4.** Cyclic voltammogram of the modified electrodes in an electrolyte of 150 g/L H<sub>2</sub>SO<sub>4</sub> and 65 g/L Zn<sup>2+</sup> (scan rate: 10 mV/s)

3.4.2. Anodic polarization curves and kinetic parameters of modified electrode for oxygen evolution reaction



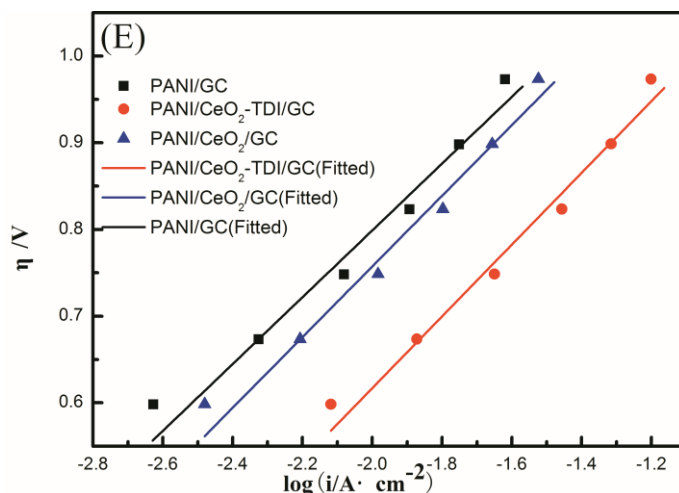


**Figure 5.** Anodic polarization curves of electrodes in an electrolyte of 150 g/L H<sub>2</sub>SO<sub>4</sub> and 65 g/L Zn<sup>2+</sup>, PANI/GC (A), PANI/CeO<sub>2</sub>-TDI/GC (B) and PANI/CeO<sub>2</sub>/GC (C) (Scan rate: 10 mV/s) recorded at various rates (0~1800 rpm). (D) is the Anodic polarization curves of modified electrode at rate of 1500 rpm, and (E) Tafel plot of modified electrode for oxygen evolution reaction at rate of 1500 rpm

Oxygen evolution activity of modified electrodes is characterized by anodic polarization using RDE with a scan rate of 10 mVs<sup>-1</sup> in an electrolyte of 150 g/L H<sub>2</sub>SO<sub>4</sub> and 65 g/L Zn<sup>2+</sup>. Fig 5 (A), (B) and (C) show the well defined anodic polarization curves in the potential window of 0~2.0 V. Meanwhile, the electrocatalytic activity of oxygen evolution is characterized in 500 A/m<sup>2</sup>. It can be seen the oxygen evolution potential decreases when the rotation rate is increased from 0 to 1800 rpm. However, when the speed reaches to 1500 rpm, the potential of oxygen evolution doesn't decline remarkably with the speed increasing. This phenomenon suggests that the oxygen evolution reaction (OER) at the modified electrode is limited by kinetic control. Therefore, the kinetics of OER are obtainable from Figure 5D and Figure 5E.

Table 1 shows the oxygen evolution potential of different electrodes at the different speed. The oxygen evolution potentials of PANI/GC, PANI/CeO<sub>2</sub>-TDI/GC, and PANI/CeO<sub>2</sub>/GC at the static moment are 1.92 V, 1.78 V, and 1.84 V, respectively. Compared with PANI/GC and PANI/CeO<sub>2</sub>/GC, evolution potential of PANI/CeO<sub>2</sub>-TDI/GC at different speed is always the lowest, which suggests that OER activity of the catalysts is in such order, PANI/CeO<sub>2</sub>-TDI/GC>PANI/CeO<sub>2</sub>/GC>PANI/GC.

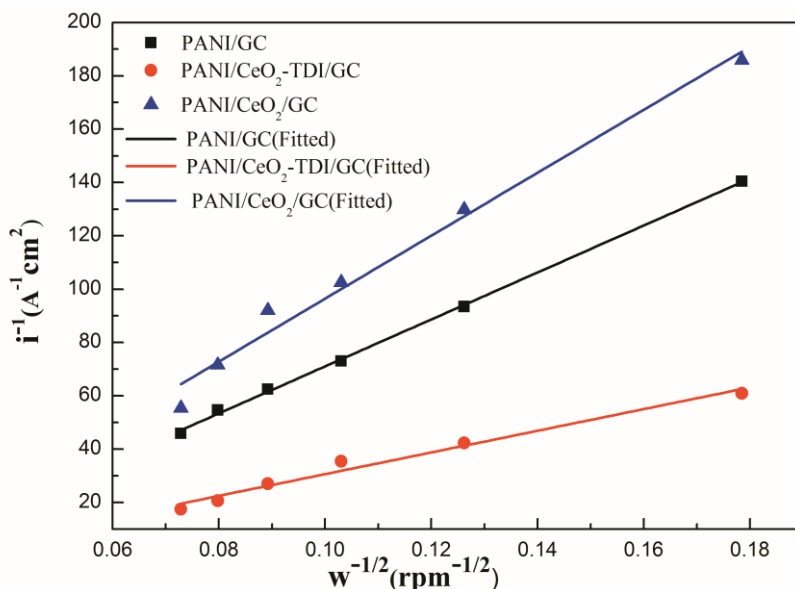
**Table 1** Oxygen evolution potential of Modified electrode at different speed (j=0.05 A/cm<sup>2</sup>)

Modified electrode	φ(O <sub>2</sub> )/V						
	0 rpm	300 rpm	600 rpm	900 rpm	1200 rpm	1500 rpm	1800 rpm
PANI/GC	1.92	1.87	1.82	1.78	1.78	1.76	1.73
PANI/CeO <sub>2</sub> -TDI/GC	1.78	1.72	1.68	1.65	1.58	1.52	1.50
PANI/CeO <sub>2</sub> /GC	1.84	1.78	1.75	1.74	1.72	1.70	1.66

**Table 2** Oxygen evolution kinetic parameters of modified electrode at rate of 1500 rpm

Modified electrode	Tafel formula parameters		
	a	b	$i_0$ ( $A \cdot cm^{-2}$ )
PANI/GC	1.57	0.38	$7.3 \times 10^{-5}$
PANI/CeO <sub>2</sub> -TDI/GC	1.45	0.41	$2.9 \times 10^{-4}$
PANI/CeO <sub>2</sub> /GC	1.56	0.40	$1.2 \times 10^{-4}$

According to Figure 5E and Table 1, kinetic parameters of OER at the rotation rate of 1500 rpm for modified electrodes are listed Table 2, which were calculated by the Tafel formula ( $\eta = a + b \cdot \log(i)$ ). The overpotential ( $\eta$ ) is calculated by equation  $\eta = E + 0.64 - 1.241 \cdot i \cdot R_s$ , where E stands for potential of oxygen evolution (between 1.45 V-1.6 V), 0.64 V the potential of the MSE, 1.241 V equilibrium potential and  $i \cdot R_s$  the electrolyte potential between the reference and working electrodes. Further insight into the kinetics of OER at modified electrode was obtained by an analysis of Table 2. The electrode surface current density for PANI/CeO<sub>2</sub>-TDI/GC modified electrode is higher ( $2.9 \times 10^{-4} A \cdot cm^{-2}$ ) than that of the other two modified electrodes, which indicates that the electrode reaction occurs faster. Therefore, PANI and CeO<sub>2</sub> can achieve a significant synergistic effect by using TDI as intermediate.

**Figure 6.** The Koutecky-Levich plots of modified electrodes ( $E=1.4$  V)

In Koutecky-Levich equation  $\{i^{-1} = (nAFKC)^{-1} + 1.61(nAFC)^{-1}D^{-2/3}v^{1/6}\omega^{-1/2}\}$  [17], the reaction rate constant(K) is very important to further verify the related oxygen evolution kinetics parameters of PANI/CeO<sub>2</sub>-TDI. For other parameters, the variable  $i$  is the measured current density, F Faraday constant,  $n(=4)$  the number of electrons that OH<sup>-</sup> ions participate in the reaction transfer, D diffusion coefficient of OH<sup>-</sup> ions in ZnSO<sub>4</sub> solution, A surface area of the disk electrode,  $v$  kinematic viscosity coefficient of ZnSO<sub>4</sub> solution, C solubility of OH<sup>-</sup> in the electrolyte. Figure 6 shows the Koutecky-

Levich plots of modified electrodes at 1.4 V. The curves indicate that  $1/i$  vs.  $\omega^{-1/2}$  is linear, and the intercepts of the plots are used to determine the kinetic parameters, which are shown in Table 3. From the last column of Table 3, it can be seen that the reaction rate constant of OER at the PANI/CeO<sub>2</sub>-TDI/GC modified electrode is the largest, displaying that in the absence of mass-transfer effects, the reaction is the fastest, which is accordant with result form anode polarization curves.

**Table 3** Verification of Koutecky-Levich equation

Modified electrode	Koutecky-Levich equation: $(nAFKC)^{-1} + 1.61(nAFC)^{-1}D^{-2/3}v^{1/6}\omega^{-1/2}$						
	nF (10 <sup>5</sup> C/mol)	C (10 <sup>15</sup> M)	A (10 <sup>-5</sup> m <sup>2</sup> )	N (10 <sup>-9</sup> m <sup>2</sup> /s)	Intercept	Slope	K x10 <sup>11</sup>
PANI/GC	3.86	9.54	1.96	8.97	17.04	880.86	8.13
PANI/CeO <sub>2</sub> -TDI/GC	3.86	9.54	1.96	8.97	10.03	406.67	13.9
PANI/CeO <sub>2</sub> /GC	3.86	9.54	1.96	8.97	21.63	1180.74	6.61

3.5. Mechanism of grafting polymerization

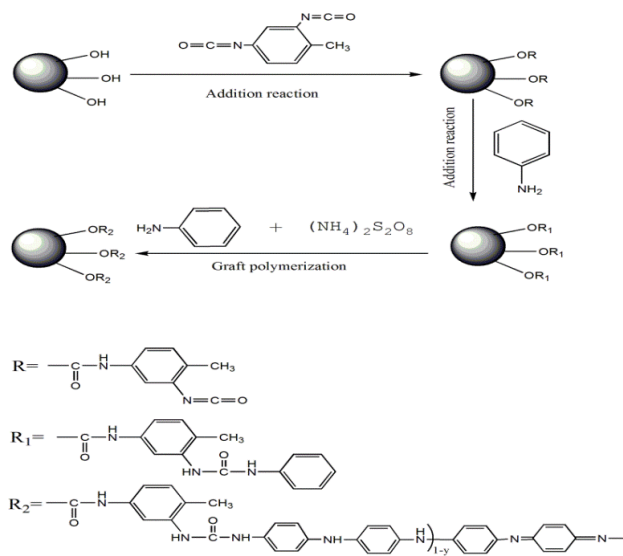


**Figure 7.** The Scheme of Preparation of PANI/CeO<sub>2</sub>-TDI

The scheme of PANI/CeO<sub>2</sub>-TDI composites synthesis is shown in Figure 7. The graft polymerization includes two steps, surface activation, and graft polymerization. In the former step, hydroxyl groups at the surface of CeO<sub>2</sub> particles react with the para-isocyanate groups and leave unreacted the ortho-isocyanate groups in TDI molecules because of their different reactivity and steric hindrance in the TDI molecule[18], and all the hydroxyl groups at the CeO<sub>2</sub> surface can be covered by isocyanate groups, which provides a method for forming covalent bonds between N atoms in the

polymerization monomers and the isocyanate groups at the CeO<sub>2</sub> surface. Those covalent bonds build the OCONH- bridges between the TDI molecules and inorganic particles. Secondly, the aniline is grafted onto the surface of CeO<sub>2</sub> via the addition reaction between an ortho-isocyanate group on CeO<sub>2</sub> and an amino group in aniline. Therefore, polymerization starts from the activity of modified particles while adding into oxidant, then aniline dimer and aniline trimer would be regularly polymerized on the CeO<sub>2</sub> particle surface.

### 3.6 Comparison of PANI based composites used as anode materials

The potentials of oxygen evolution reaction for different anode materials in the acidic environment are summarized in Table 4. Compared with inorganic coatings and other PANI based composites, it's obvious that PANI-CeO<sub>2</sub>-TDI has the lowest OER potential.

**Table 4.** Potential of OER of coatings for zinc electrowinning

Anode materials	Potential of OER in a 150 g/L H <sub>2</sub> SO <sub>4</sub> when current density is 50 mA/cm <sup>2</sup> , (V, vs SHE)
PANI-CeO <sub>2</sub> -TDI (this work)	1.140
PANI-CeO <sub>2</sub> (this work)	1.196
RuO <sub>2</sub> Coating [19]	1.641
PANI-WC [20]	1.757
PbO <sub>2</sub> Coating [19]	2.177

## 4. CONCLUSIONS

We prepared the unreported PANI/TDI-CeO<sub>2</sub> composite via graft polymerization. In its FTIR spectrum that all the peaks showed blue shifts indicates there is strengthened interaction between CeO<sub>2</sub>-TDI and PANI. In the XRD spectrum of CeO<sub>2</sub>-TDI, the diffraction pattern is the same with that of pristine CeO<sub>2</sub>, which implies that crystal structure of CeO<sub>2</sub> particles isn't affected by TDI modification, but polyaniline coated on the unmodified CeO<sub>2</sub> will affect the crystal form of CeO<sub>2</sub> because the peak of CeO<sub>2</sub> disappears in XRD spectrum of composite PANI/CeO<sub>2</sub>. In the TGA curve of PANI/CeO<sub>2</sub>-TDI, the mass loss of PANI/CeO<sub>2</sub>-TDI begins at about 260 °C which is the highest among the tested samples, showing excellent thermostability. In the CV curves, the peak current of PANI/CeO<sub>2</sub>/GC electrode is higher than that of PANI/GC electrode, indicating that the inorganic particles CeO<sub>2</sub> will affect both the electrocatalytic conductivity and capacitance characteristics of PANI. From the CV curve of PANI/CeO<sub>2</sub>-TDI/GC modified electrode, it can be seen larger peak current and better electrochemical activity when referred to that of PANI/GC modified electrode, indicating that TDI within the composites can improve the performance of pure PANI. From the OER curves, it can be seen the oxygen evolution potential decreases when the rotation rate is increased from 0 to 1800 rpm, while when the speed reaches to 1500 rpm, the potential of oxygen evolution doesn't

decline remarkably with speed increasing. This fact suggests that the OER at the modified electrode is limited by kinetic control. By comparison, we obtained the OER activity order of PANI/CeO<sub>2</sub>-TDI/GC>PANI/CeO<sub>2</sub>/GC>PANI/GC. The electrode surface current density and the reaction rate constant for PANI/CeO<sub>2</sub>-TDI/GC modified electrode are the highest ( $2.9 \times 10^{-4} \text{ A} \cdot \text{cm}^{-2}$  and  $1.39 \times 10^{12}$ , respectively) among three modified electrodes. Finally, a possible mechanism of the graft polymerization is that aniline is grafted onto the surface of CeO<sub>2</sub> via the addition reaction between an ortho-isocyanate group on CeO<sub>2</sub> and the amino group in aniline, which initiates the polymerization and then aniline dimer and aniline trimer would be regularly polymerized on the TDI-CeO<sub>2</sub> particle's surface.

#### ACKNOWLEDGEMENTS

This research was supported by the National Natural Science Foundation of China (No. 51504111) and the applied basic research plan on the project in Yunnan province (Nos. 2013FA012 and 2013FB022). The authors are grateful to Prof. H. Huang, Prof. Z.C. Guo and Dr. B.M. Cheng for their helpful advices during the preparation of this paper.

#### References

1. T. A. Skotheim, *Crc Press* (1997).
2. G. Cui, J. S. Lee, S. J. Kim, H. Nam, G.S. Cha, H.D. Kim, *Analyst*, 123 (1998) 1855.
3. A. A. Karyakin, M. Vuki, L.V. Lukachova, E.E. Karyakina, A.V. Orlov, G.P. Karpachova, J. Wang, *Analytical Chemistry*, 71 (1999) 2534.
4. M. M. Ayad, N. Salahuddin, M.A, *Synthetic Metals*, 132 (2003)185.
5. J. Kašpar, P. Fornasiero, M. Graziani, *Catalysis Today*, 50 (1999)285.
6. Q. Fu, S. Kudriavtseva, H. Saltsburg, *Chemical Engineering Journal*, 93 (2003)41.
7. Q. Fu, H. Saltsburg, M. Flytzani-Stephanopoulos, *Advances in Medical & Dental Sciences*, 5635 (2003) 935.
8. H. -J. BeieA. Gnö. *Sensors & Actuators B Chemical* 4.3-4 (1991):393-399.
9. A. Lipińska, P. Sautière, G. Biserte, *Journal of Materials Science*, 20 (2012)7148.
10. J. Q. Zhang, Y. Q. Song, Y.J. Geng, *Chinese Rare Earths*, 35 (2014)82.
11. F. Y. Chuang, S. M. Yang, *Journal of Colloid and Interface Science*, 320 (2008) 194.
12. B. Ou, D. Li, Q. Liu, Z. Zhou, G. Chen, P. Liu, *Journal of Macromolecular Science, Part A: Pure and Applied Chemistry*, 49 (2012)149.
13. M. E. Jozefowicz, A.J. Epstein, J. P. Pouget, J. G. Masters, A. Ray, A. G. Macdiarmid, *International Journal of Biological Macromolecules*, 24 (1991) 5863.
14. G.K. Paul, A. Bhaumik, A.S. Patra, S.K. Bera, *Materials Chemistry & Physics*, 106 (2007) 360.
15. L.T. Cai, S.B. Yao, S.M. Zhou, *Journal of Electroanalytical Chemistry*, 421 (1997) 45.
16. F. J. Haftka, E. Votava, *Journal of Materials Science Letters*, 34 (1999) 2733.
17. Bard AJ, Faulkner LR, *Wiley*, 2001.
18. Li S, Liu Y., *Beijing:Chemical Industry Press*, (1998).
19. M. Taguchi, H. Takahashi, T. Takahashi, *Journal of Mmij*, 132 (2016) (3) 59.
20. R. Xu, Y. Guan, H. Chen, L. Huang, P. Zhan, *Journal of the Chinese Advanced Materials Society*, 1 (2013) (1) 40.